Hydrocarbon and Carbon Nanostructures Produced by Sonochemical Reactions of Organic Solvents on Hydrogen-Passivated Silicon Nanowires under Ambient Conditions

C. P. Li,[†,‡] Boon K. Teo,*[,§] X. H. Sun,[†,||,⊥] N. B. Wong,[†,||] and S. T. Lee*[,†,‡]

Center of Super-Diamond & Advanced Film, Department of Physics and Materials Science, and Department of Biology and Chemistry, City University of Hong Kong, Hong Kong SAR, China, and Department of Chemistry, University of Illinois at Chicago, 845 W. Taylor Street, Chicago, Illinois 60607

Received February 16, 2005. Revised Manuscript Received September 7, 2005

A simple sonochemical solution method using silicon nanowires (SiNWs) as templates has been developed to synthesize a wide variety of carbon nanostructures under ambient conditions (room temperature and atmosphere pressure). In addition to the conventional carbon nanotubes (CNTs) and nano-onions (CNOs), with interlayer spacings of 3.4 Å, a new class of hydrocarbon nanostructures, characterized as hydrocarbon nanotubes (HCNTs) and nano-onions (HCNOs), which exhibit variable interlayer spacings greater than 3.4 Å, has been discovered. A wide variety of morphologies of these hydrocarbon nanostructures were observed, including, but not limited to, tubes (both solid and hollow tubes); onions (both solid and hollow onions); tubular networks; open, closed, or connected loops or other networks; and twisted tubes or loops. Strong evidence for the templating effect of the SiNWs, including the molding and the demolding (extrusion) processes, were provided by direct transmission electron microscopic observations. The structure and bonding characteristics of this class of hydrocarbon nanomaterials were probed by single-nanowire electron-energy-loss spectroscopy and Raman spectroscopy. The distinctive properties of the hydrocarbon nanotubes and nano-onions, which are different from those of the conventional carbon nanotubes and nano-onions, are also discussed. Based on these experimental observations, mechanistic pathways for the formation of these nanostructures are proposed.

Introduction

The unusual electronic, optical, and mechanical properties of fullerenes,[1] nanotubes,[2,3] and nano-onions[4] make them topics of intensive investigations. Among the commonly used techniques for producing carbon nanotubes (CNTs) and nano-onions (CNOs) are arc discharge,[2] laser ablation,[5] chemical vapor deposition (CVD),[6] electron beam irradiation and high-temperature annealing,[4,7] etc. Most of these techniques require such severe conditions as high temperature, high vacuum, high voltage arc discharge, or high-energy electron irradiation. Some also require specialized equipment such as lasers and CVD or metal catalysts, though an interesting report of the synthesis of CNTs[8] and CNOs[9] by arc discharge (using graphite electrodes) in water at room temperature has appeared. Recently, we reported in a communication[10] a simple sonochemical solution method using silicon nanowires (SiNWs) as templates to produce a wide variety of carbon nanostructures in common organic solvents, using an ordinary laboratory sonicator, under ambient conditions (room temperature and atmosphere pressure). This technique is extremely simple; it requires neither specialized equipment nor metal catalysts. After our communication,[10] a report of a similar sonication method in *p*-xylene for the synthesis of single-walled carbon nanotubes on the surface of the silica powder appeared.[11] The latter, however, requires ferrocene as the precursor of Fe catalyst and silica powder as the nucleation site.

The carbon nanostructures produced by our method, in the forms of nanotubes and nano-onions, have interlayer spacings ranging from 3.4 to 5.9 Å. The products can be categorized into two broad classes: the conventional carbon nanotubes (CNTs) and nano-onions (CNOs), on one hand, and a new class of carbon nanomaterials which may be termed hydrocarbon nanotubes (HCNTs) and nano-onions (HCNOs), on the other hand. The former has the expected

* To whom correspondence should be addressed. E-mail: boonkteo@uic.edu (Boon K. Teo); apannale@cityu.edu.hk (S. T. Lee).
† Center of Super-Diamond & Advanced Film, City University of Hong Kong.
‡ Department of Physics and Materials Science, City University of Hong Kong.
§ Department of Chemistry, University of Illinois at Chicago.
|| Department of Biology and Chemistry, City University of Hong Kong.
⊥ Present address: Department of Chemistry, University of Western Ontario, London, Canada.

(1) Kroto, H. W.; Heath, J. R.; O'Brien, S. C.; Curl, R. F.; Smalley, R. E. *Nature* **1985**, *318*, 162−163.
(2) Iijima, S. *Nature* **1991**, *354*, 56−58.
(3) Iijima, S.; Ichihashi, T. *Nature* **1993**, *363*, 603−605.
(4) Ugarte, D. *Nature* **1992**, *359*, 707−709.
(5) Thess, A.; Lee, R.; Nikolaev, P.; Dai, H. J.; Petit, P.; Robert, J.; Xu, C. H.; Lee, Y. H.; Kim, S. G.; Rinzler, A. G.; Colbert, D. T.; Scuseria, G. E.; Tomanek, D.; Fischer, J. E.; Smalley, R. E. *Science* **1996**, *273*, 483−487.
(6) Kong, J.; Cassell, A. M.; Dai, H. J. *Chem. Phys. Lett.* **1998**, *292*, 567−574.
(7) De Heer, W. A.; Ugarte, D. *Chem. Phys. Lett.* **1993**, *207*, 480−486.
(8) Hsin, Y. L.; Hwang, K. C.; Chen, F. R.; Kai, J. J. *Adv. Mater.* **2001**, *13*, 830−833.
(9) Sano, N.; Wang, H.; Chhowalla, M.; Alexandrou, I.; Amaratunga, G. A. J. *Nature* **2001**, *414*, 505−506.
(10) Sun, X. H.; Li, C. P.; Wong, N. B.; Lee, C. S.; Lee, S. T.; Teo, B. K. *J. Am. Chem. Soc.* **2002**, *124*, 14856−14857.
(11) Jeong, S.-H.; Ko, J.-H.; Park, J.-B.; Park, W. *J. Am. Chem. Soc.* **2004**, *126*, 15982−15983.

10.1021/cm050355n CCC: $30.25
Published on Web 10/19/2005

interlayer spacings of 3.4 Å while the latter exhibits variable interlayer spacings ranging from 3.4 to 5.9 Å. Since many common organic solvents can be used and SiNWs can be produced in large quantities, this simple synthetic route to CNT/HCNT and CNO/HCNO opens the door to economical preparation of large quantities of these nanomaterials.

The SiNWs are one-dimensional nanowires of crystalline silicon, which can be synthesized by thermal evaporation of SiO[12] or by laser ablation of metal-containing silicon targets.[13] The SiNWs used in this work were prepared by thermal evaporation of SiO method and contained no metal catalysts. The as-synthesized SiNWs have a thick silicon oxide sheathing.[12] The oxide sheathing can be removed by a controlled HF treatment. The surfaces of the HF-etched SiNWs have been found to be passivated by hydrogen (i.e., SiH_x species, where $x = 1-3$) and exhibit moderately high reactivity in solution.[14−17] In fact, it was during an attempt to disperse oxide-free SiNWs in common organic solvents that we discovered this new type of well-structured, hydrocarbon nanomaterials.

We report herein details of the preparation, characterization, and properties of this new type of carbon nanomaterials. Direct transmission electron microscopic observations, in addition to revealing a wide variety of morphologies, provide strong evidence for the templating effect of the SiNWs, including the molding and the demolding (extrusion) processes, in the formation of these nanomaterials. The structure and bonding characteristics of this class of hydrocarbon nanomaterials were probed by single-nanowire electron energy loss spectroscopy and Raman spectroscopy. The reaction mechanism and the formation pathways are also proposed.

Experimental Section

SiNWs were synthesized by thermal evaporation of SiO powders. SiNWs were oxide-removed and H-passivated by etching with an aqueous (5%) HF solution. The new HCNTs and HCNOs can be produced by dispersing HF-etched SiNWs in certain common solvents such as $CHCl_3$, CH_2Cl_2, and CH_3I, followed by bath sonication for 15 min in a common laboratory ultrasonic cleaner (40 kHz) under ambient conditions (room temperature and pressure). The golden yellowish solution turned turbid within minutes of sonication and exhibited Tyndal effect characteristic of colloidal solutions. A few drops of the resulting solution were put onto a lacey carbon film and characterized by high-resolution transmission electron microscopy (HRTEM, Philips CM200 FEG, operated at 200 keV), electron energy loss spectroscopy (EELS), and elemental mapping (Gatan GIF 200), which were attached to the HRTEM operating at 200 kV.

The sample for Raman study was prepared as follows. A relatively large quantity of SiNWs (1 mg) was dispersed in 2 mL of $CHCl_3$ after HF treatment by the same procedure as previously described. The solution was dropped onto a glass slide and dried in the air. This procedure was repeated many times until approximately 1 mL solution was evaporated to produce a thin solid film of 1 cm in diameter. Within the film, small bundles of SiNWs were observed. The sample was subsequently examined by Raman spectroscopy using a Renishaw micro-Raman spectrometer at room temperature. Excitation was by means of the 514 nm line of an Ar^+ laser, and the Raman signals were measured in a backscattering geometry with a spectral resolution of 1.0 cm^{-1}.

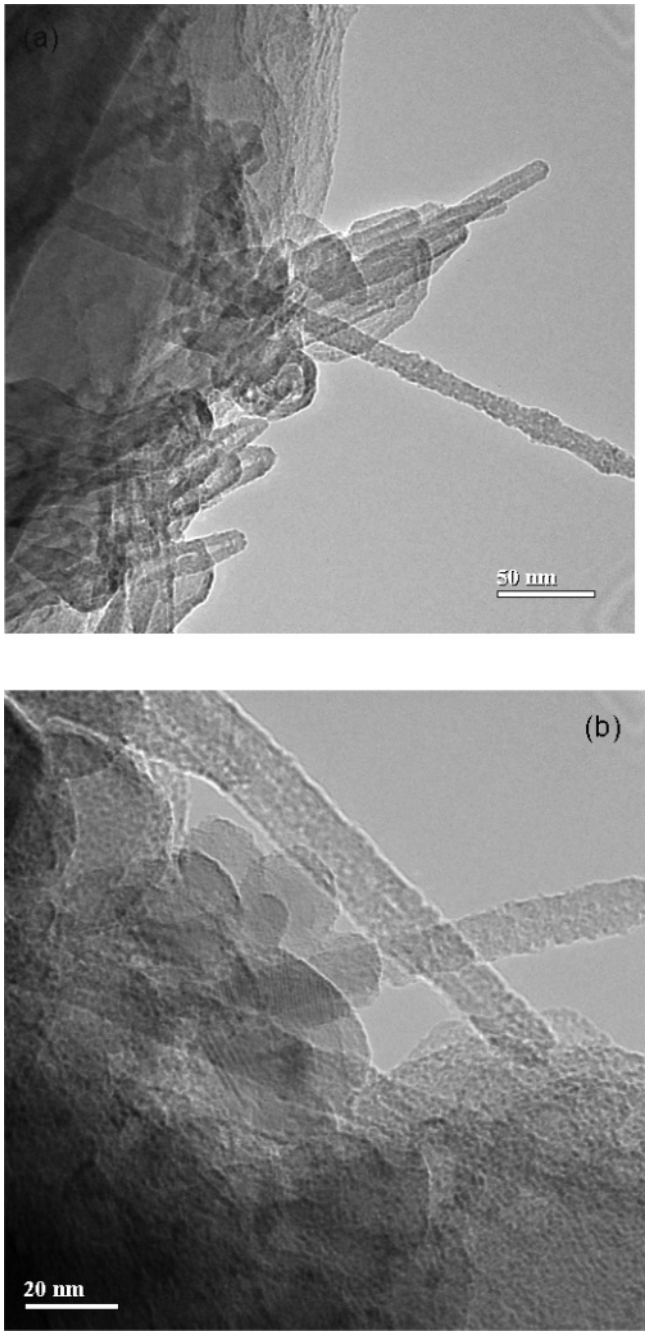

Figure 1. Low-resolution TEM images of assortments of hydrocarbon nanotubes (HCNTs) and conventional carbon nanotubes (CNTs) synthesized in $CHCl_3$ solution: (a) contains more CNTs than HCNTs; (b) contains more HCNTs than CNTs.

Results and Discussions

I. Morphological Characterization. Figures 1a and 1b are two low-magnification TEM images of the products

(12) Shi, W. S.; Peng, H. Y.; Zheng, Y. F.; Wang, N.; Shang, N. G.; Pan, Z. W.; Lee, C. S.; Lee, S. T. *Adv. Mater.* **2000**, *12*, 1343−1345.
(13) Morales, A. M.; Lieber, C. M. *Science* **1998**, *279*, 208−211.
(14) Sun, X. H.; Wang, S. D.; Wong, N. B.; Ma, D. D. D.; Lee, S. T.; Teo, B. K. *Inorg. Chem.* **2003**, *42*, 2398−2404.
(15) Sun, X. H.; Peng, H. Y.; Tang, Y. H.; Shi, W. S.; Wong, N. B.; Lee, C. S.; Lee, S. T.; Sham, T. K. *J. Appl. Phys.* **2001**, *89*, 6396−6398.
(16) Sun, X. H.; Wong, N. B.; Li, C. P.; Lee, S. T.; Kim, P. G.; Sham, T. K. *Chem. Mater.* **2004**, *16*, 1143−1152.
(17) Sun, X. H.; Li, C. P.; Wong, N. B.; Lee, C. S.; Lee, S. T.; Teo, B. K. *Inorg. Chem.* **2002**, *41*, 4331−4336.

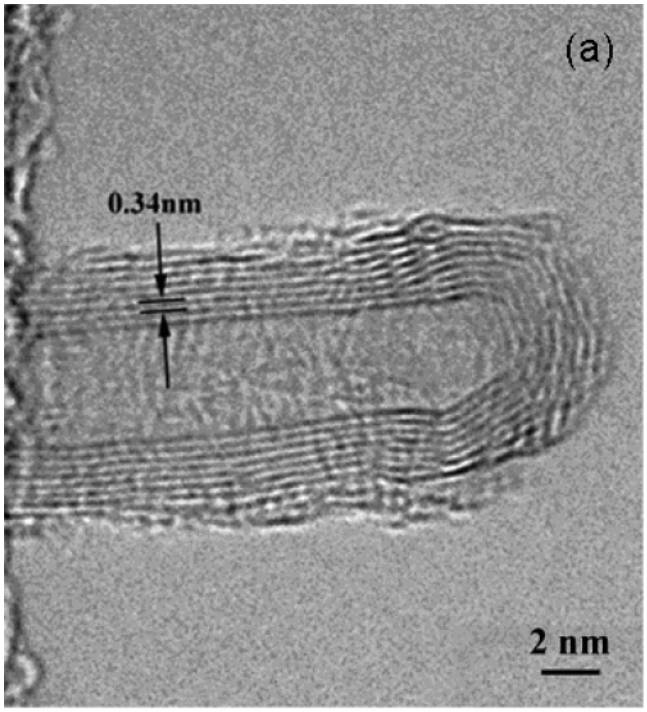

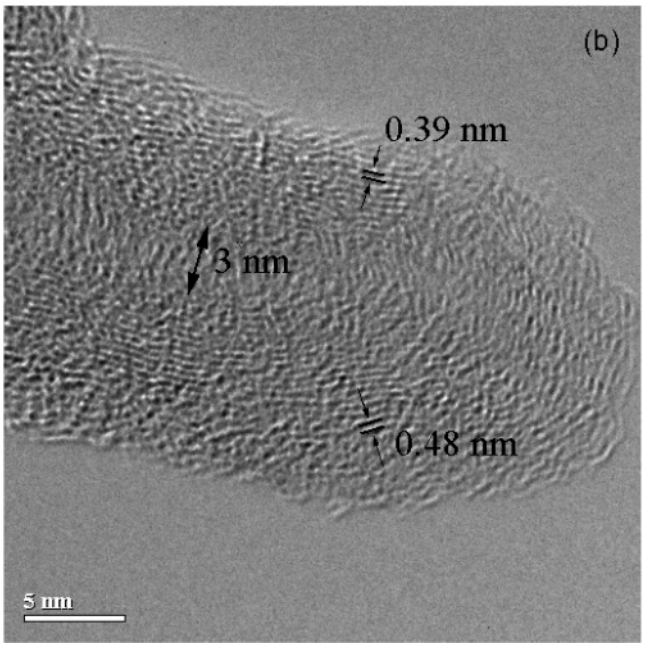

Figure 2. (a) A high-resolution TEM (HRTEM) image of a typical CNT with interlayer spacing of 3.4 Å and 8 walls. (b) A HRTEM image of a typical HCNT with inner and outer diameters of 3 and 18 nm, respectively. Both nanotubes were close-ended after extrusion from the SiNWs (the "molds").

dispersed in $CHCl_3$ and put onto holey carbon grids. As can be seen, in addition to the commonly observed CNTs with interlayer spacings of 3.4 Å, a new class of hydrocarbon (HC) nanostructures exemplified by hydrocarbon nanotubes (HCNTs) and hydrocarbon nano-onions (HCNOs), with interlayer spacings varying from 3.9 to 5.9 Å, was observed. These CNTs or HCNTs have typical diameters of about 10 nm and length of hundreds of nanometers or more. These nanostructures exhibit many shapes and forms, the most common ones being multiwall hydrocarbon nanotubes (MWHCNTs). It is apparent that Figure 1a exhibits more HCNTs than CNTs while the reverse is true for Figure 1b. Most of the CNTs have a close cap at one end and without any encapsulated metal catalysts.

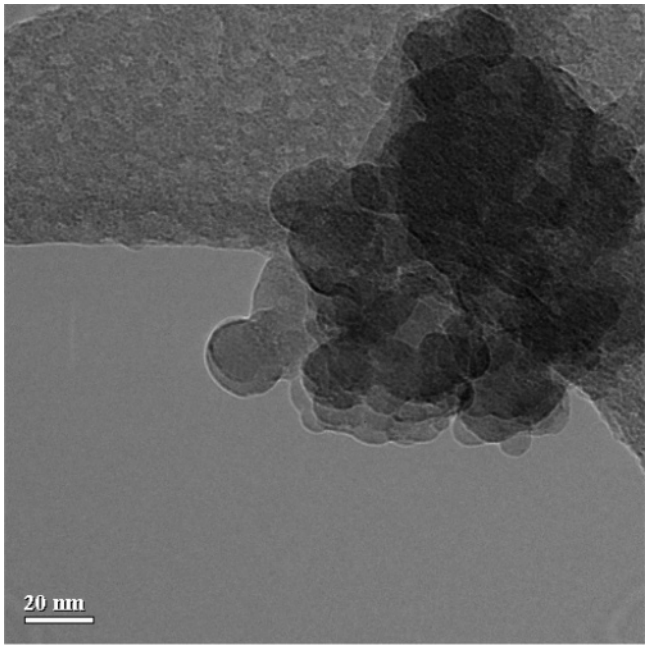

Figure 3. A low-resolution TEM image of large quantities of hydrocarbon and carbon nanoonions of tens of nanometers in diameter.

Figure 2a depicts a typical CNT which has at least 8 layers, and outer and inner diameters of 9 and 4 nm, respectively. The interlayer spacing is 3.4 Å, which matches exactly the {0002} lattice spacing of graphite and is the distinctive signature of CNT. The HRTEM image of a typical hydrocarbon nanotube (HCNT) is shown in Figure 2b. This multiwalled HCNT has an outer diameter of 15 nm and an inner diameter of 3 nm. Unlike the conventional CNTs, HCNTs have wavy layers and interlayer spacings of 3.9−4.8 Å which are distinctly different from that of 3.4 Å expected for conventional CNTs. Most of these CNTs and HCNTs are *hollow* nanotubes, though some were still attached to the silicon nanowire templates (i.e., the carbon or hydrocarbon nanotubes were filled with silicon nanowires). In addition to CNTs and HCNTs, onion-like carbon nanostructures (CNOs and HCNOs) were also observed in the products. Figure 3 shows a typical TEM image of clusters of hydrocarbon and carbon nano-onions measuring tens of nanometers in diameter. Figure 4a shows typical HRTEM images of CNOs having a core diameter of about 9 Å and approximately 13 layers. The outer diameter ranges from 10 to 20 nm, with up to 30 shells. Smaller CNOs seem to be more spherical in shape. As with the CNT, the CNOs also have interlayer spacings of 3.4 Å. Again, unlike the conventional CNOs, HCNOs have wavy layers and larger interlayer spacings. The HRTEM image of a typical HCNO, with 4.0 Å interlayer spacing, is shown in Figure 4b.

In addition to conventional CNTs and CNOs (hereafter designated collectively as CNT(O)s) and the new HCNTs and HCNOs (hereafter referred to collectively as HCNT(O)s), other shapes such as twisted tubes or loops, faceted polyhedral onions, Y-shape, and other networks of HCNTs/HCNOs can also be found. These carbon nanostructures are

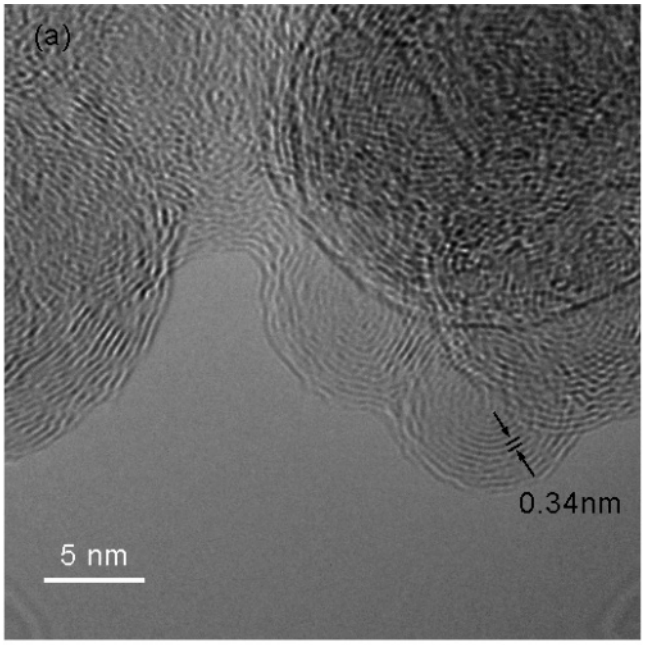

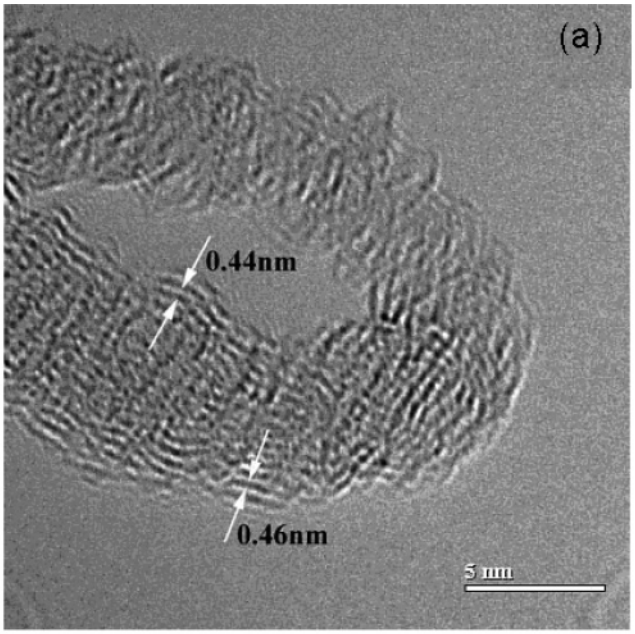

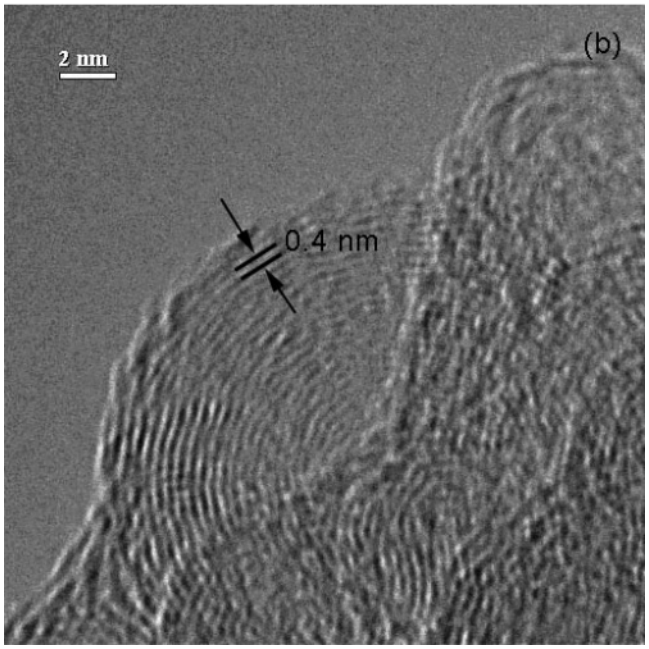

Figure 4. (a) A typical HRTEM image of CNOs with a core diameter of about 4.5 Å and interlayer spacing of 3.4 Å. (b) A HRTEM image of a HCNO, with 4.2 Å interlayer spacing.

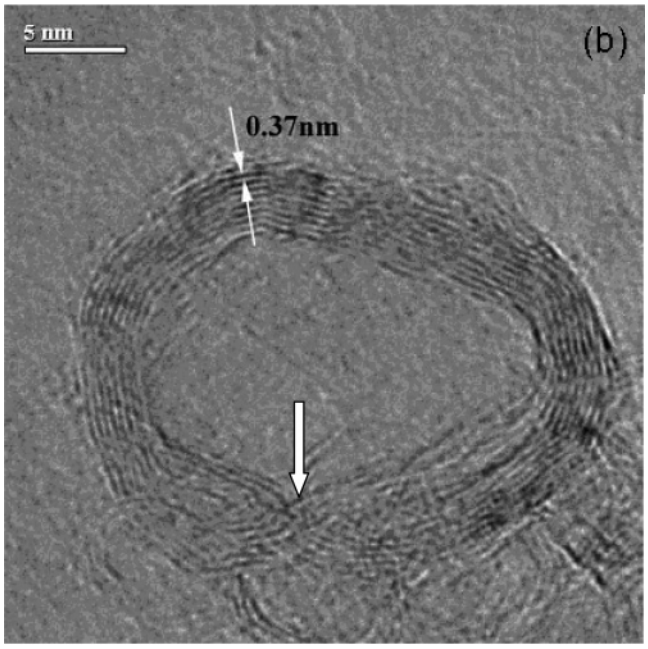

Figure 5. (a) A HRTEM image of a donut-like carbon nanoloop with 4.4 Å interlayer spacing. (b) A close-ended carbon nanoloop with 10 layers and an interlayer spacing of 3.7 Å. The unusual nanoloop in (b) can be visualized as a solid tube closed at both ends. The two closed ends are joined together, as indicated by the large arrow.

different from the conventional CNTs and CNOs in that they all have rough, wavy layers and were easily shrunk, collapsed, or damaged by the electron beam under TEM. Nonetheless, these HCNTs/HCNOs exhibit well-structured morphologies. TEM images of some representative members of these nanostructures are portrayed in Figures 5 and 6 as well as in the Supporting Information (Figures S1−S3). For example, Figures 5a and 5b depict HRTEM images of some of the loopike structures. In particular, Figure 5a shows a donut-like carbon nanoloop with 4.4 Å interlayer spacing. A closed-end-loop carbon nanoloop with 10 layers and an interlayer spacing of 3.7 Å is shown in Figure 5b. This unusual loop can also be visualized as a solid tube closed at both ends. The two closed ends are joined together, as indicated by the large arrow. Numerous other shapes were also observed, as exemplified by the Y-shaped hydrocarbon nanostructure, with interlayer spacing of 5.6 Å, portrayed in Figure 6. Further examples of other hydrocarbon nanostructures with different shapes can be found in Figures S1−S3.

II. Spectroscopic Characterization. We believe that these new structures of HCNTs/HCNOs are formed by networks of chair-form cyclohexane-like hexagonal structure that wrap around the SiNW templates (molds). These structures are similar to that of partially hydrogenated graphite on the one extreme and that of amorphous hydrocarbon (*a*-C:H) on the other. Morphologically, they are similar to the conventional

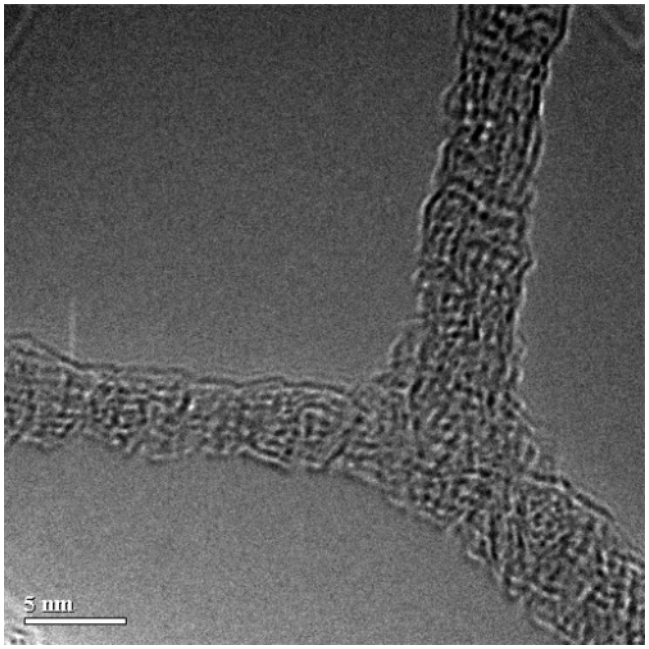

Figure 6. A HRTEM image of a Y-shape hydrocarbon nanostructure with interlayer spacing of 5.6 Å.

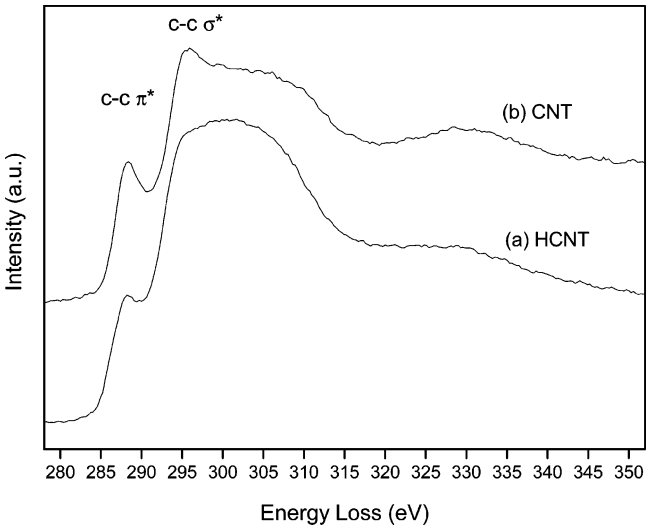

Figure 7. Representative single-nanowire EELS spectra of individual hydrocarbon nanotube (HCNT) (curve a) and carbon nanotube (CNT) (curve b).

CNTs or CNOs except that C−H bonds have been inserted between layers, thereby converting curved planar sp^2 sheets into curved puckered sp^3 sheets, or combinations thereof. The more C−H bonds inserted, the larger will be the interlayer spacings.

The *single-tube* EELS results of individual new hydrocarbon nanotube (HCNT) (curve a) and the normal carbon nanotube (CNT) (curve b), shown in Figure 7, are consistent with this notion. The main difference between the new HCNT and the conventional CNT is that HCNT exhibits less sp^2 bonds and more disordered sp^3 bonds than that in CNT as evidenced by the edge ratio sp^3 (C−C)/sp^2 (C═C) of approximately 1 for the conventional CNT but 1.5 for the new HCNT. This observation is consistent with the (partial) hydrogenation of the C═C bonds.

The Raman spectra of the products further confirmed the carbon structures are the reaction products of SiNWs and

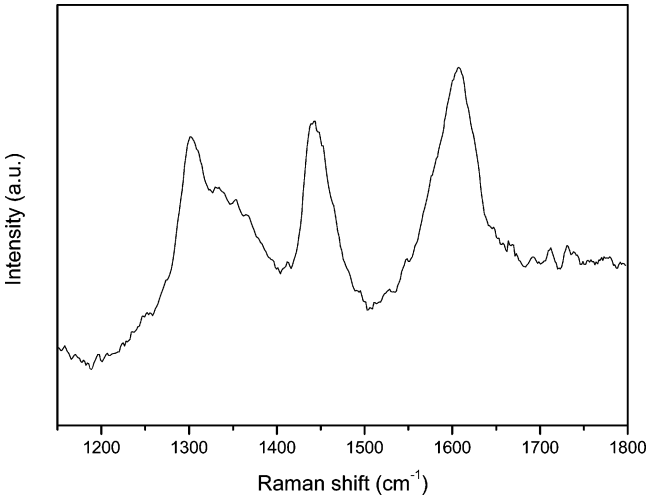

Figure 8. Raman spectra of synthesized hydrocarbon nanostructures (excitation: 514 nm line of an Ar^+ laser). A small shoulder at 1580 cm^{-1} indicates traces of conventional CNTs in the sample (see text for details).

the solvent molecules. The intense peaks at 517 and 960 cm^{-1} can be ascribed to the scattering of the first-order optical phonon and the overtone of TO (L) of Si in SiNWs, respectively. More importantly, in the range of 1100−1800 cm^{-1}, there were three weak peaks at 1300, 1450, and 1600 cm^{-1}, depicted in Figure 7. The peak at 1300 cm^{-1} can be assigned to sp^3 (C−C single bond) whereas that at 1600 cm^{-1} to sp^2 (C═C double bond) stretching frequencies of the HCNT(O)s. The peak at 1450 cm^{-1} is rather unusual and may be tentatively assigned to a carbon−carbon stretching frequency corresponding to a bond order of approximately 1.5. A careful examination of Figure 8 also revealed three weak shoulders at 1340, 1360, and 1370 cm.$^{-1}$ These bands may be attributed to the residual disordered graphite-like or amorphous carbon-like nanomaterials remaining on the outer or inner surfaces of the HCNTs or at the interfaces between the HCNTs and the SiNW templates. We note that these bands are very different from those observed for conventional CNTs which have a strong peak at 1580 cm^{-1} (sp^2), the so-called G-band tangential mode, and a much weaker peak at 1348 cm^{-1} (sp^3), the so-called D-band related to the disordered graphite and/or amorphous carbon. For comparison, the characteristic Raman peak of diamond occurs at 1332 cm^{-1}, which may be taken as the benchmark for sp^3 C−C single-bond stretching frequency.

III. Characteristics of HCNTs and HCNOs. We shall now describe the peculiar properties of HCNTs and HCNOs. The characteristics of HCNT(O)s, which distinguish them from the conventional CNT(O)s are as follows: (1) wavy layers or shells; (2) large and variable interlayer spacings ranging from 3.4 to 5.9 Å; (3) easily shrunk, buckled, damaged, or broken by intense electron beam; (4) partially hydrogenated, the degree of hydrogenation decreasing with the sonication time; (5) free of metal or other catalysts; and (6) prolonged sonication can convert HCNT(O) into CNT(O)s (vide infra). Obviously the layer morphology, the interlayer spacing, and the degree of hydrogenation are intimately related to the sp^3/sp^2 bond ratio which depends critically on the sonication time, the starting material (organic molecule), and the surface condition of the SiNW(D)

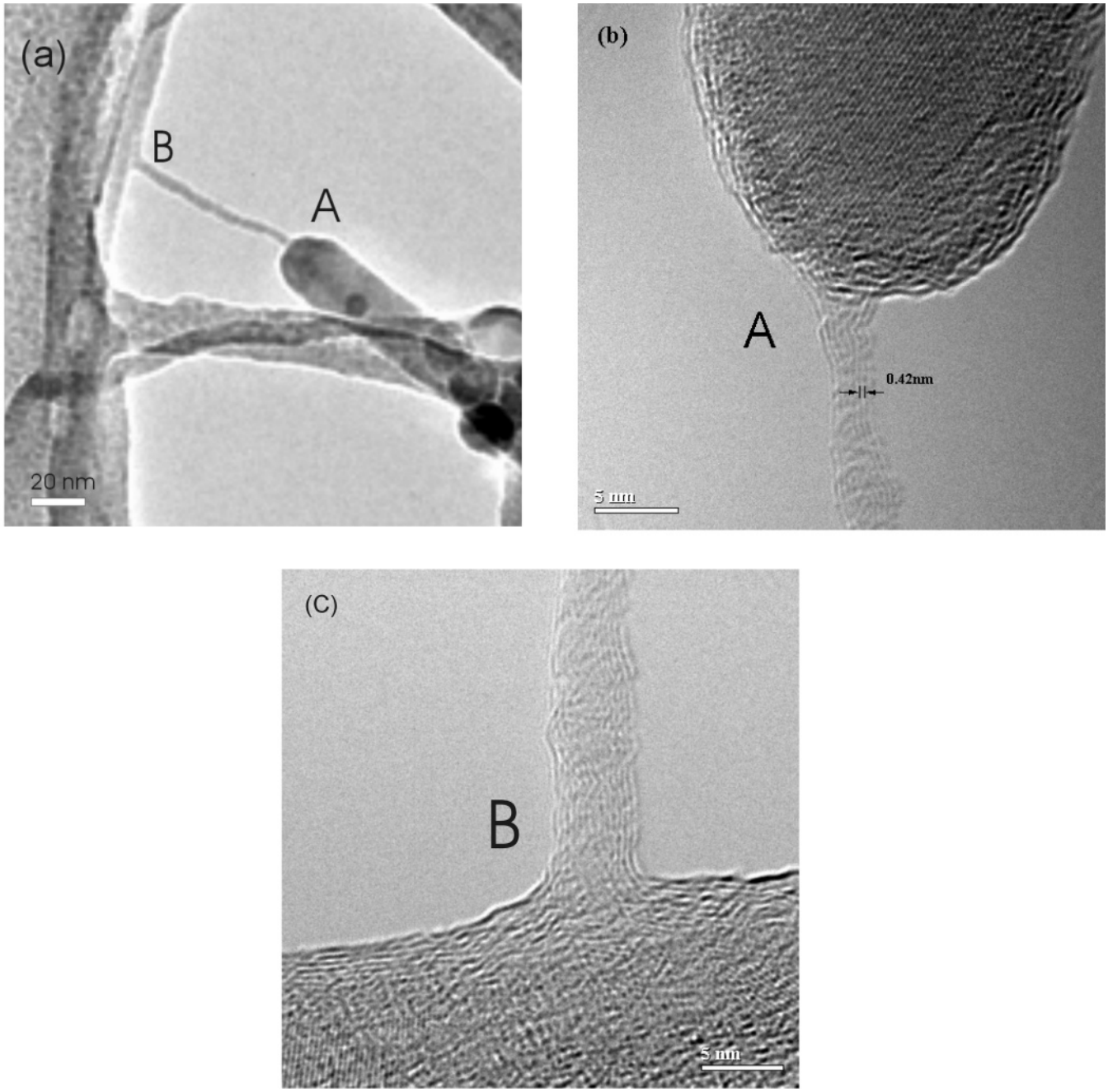

Figure 9. "Caught-in-the-act" TEM images of the extrusion process in the formation of a HCNT on a SiNW: (a) a HCNT connecting the tip of a SiNW (A) to the body of another SiNW (B). (b) HRTEM image taken from area "A" in (a). (c) HRTEM image taken from area "B" in (a).

template. Prolonged ultrasonication usually leads to better morphologies of the products with smoother layers and the eventual extrusion of the SiNW(D)s (the "molds").

We shall now discuss the implications of these characteristics and show how they relate to, and indeed provide strong evidence for, the proposed formation pathway of these carbon nanomaterials on silicon nanowire templates (vide infra).

IV. Templating: Molding and Demolding. We believe the SiNWs serve as templates for the formation of these nanostructrues, as evidenced by the "caught-in-the-act" TEM picture shown in Figure 9a. Here, a HCNT of about 4 nm in diameter and 65 nm in length was found to connect the tip of one SiNW (A) to the body of another SiNW (B). The SiNWs have diameters of about 30 nm. The EELS results, taken from area between "A" and "B", reveal that it comprises mainly of carbon. The HRTEM image in Figure 9b, taken from area "A" in Figure 9a, showed that this HCNT has an interlayer spacing of 4.2 Å, emanating from the tip of a SiNW marked A in Figure 9a. This seven-layered HCNT is connected to another SiNW marked B in Figure 9a. The expanded image of area "B" in Figure 9a is depicted in Figure 9c.

Figure 10a shows another "caught-in-the-act" TEM image of the templating effect: the extrusion of a HCNT from a SiNW. The corresponding TEM elemental mapping results are depicted in Figures 10b and 10c, which confirm the chemical compositions of the template SiNW (silicon mapping, Figure 10b) and the product HCNT (carbon mapping, Figure 10c), respectively.

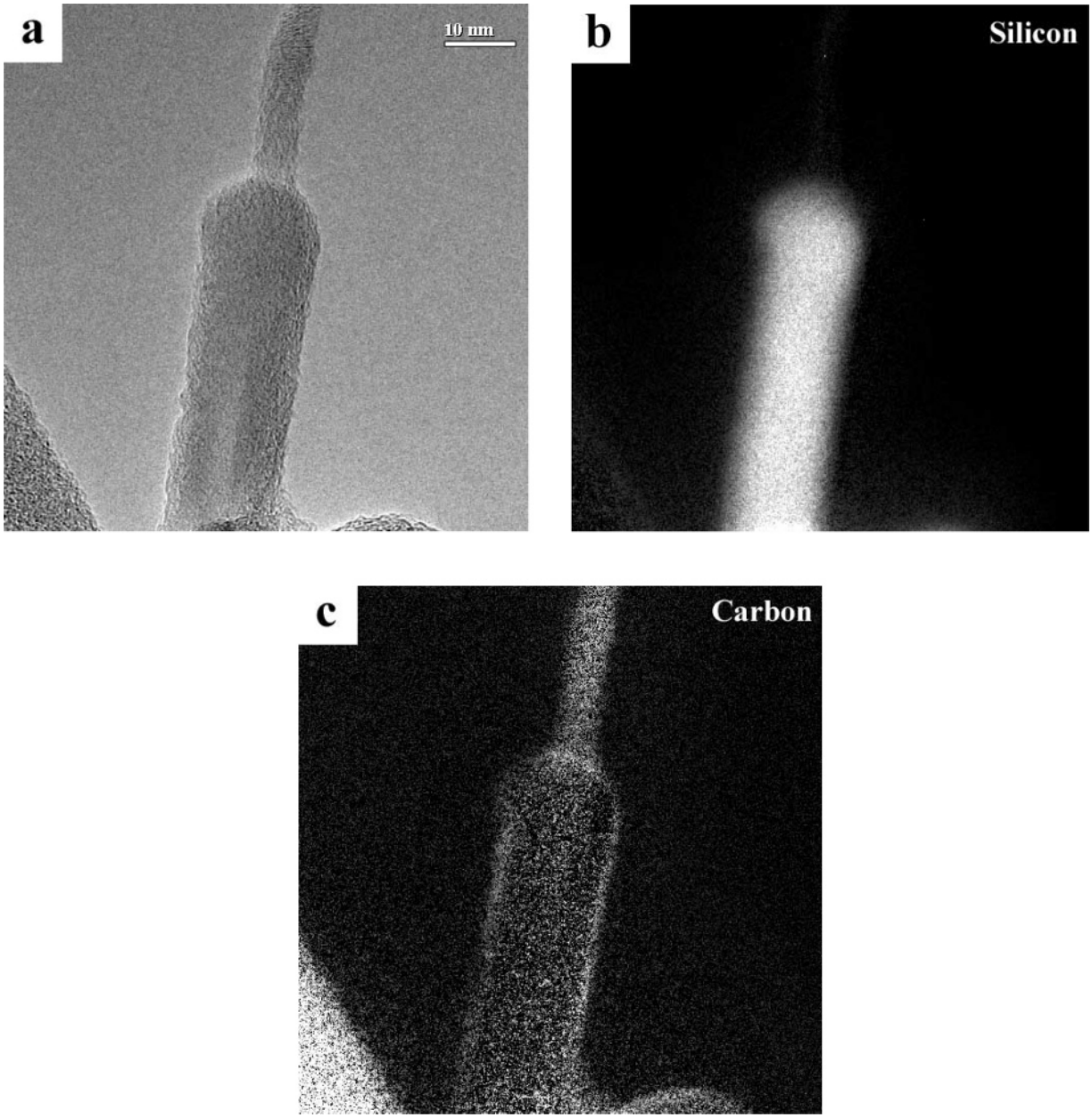

Figure 10. "Caught-in-the-act" TEM images of the templating effect: (a) the extrusion of a HCNT from a SiNW; (b) the corresponding silicon mapping; and (c) the corresponding carbon mapping.

Note that, in both Figures 9 and 10, the HCNTs collapsed immediately after extrusion (demolding) from the SiNWs (the mold).

V. Formation Pathway(s). Based on our HRTEM observations and the spectroscopic evidence, we wish to propose a reaction pathway for the formation of these new carbon nanostructures on SiNWs. We believe that the formation of these carbon nanostructures is intimately associated with active reaction sites (which also serve as nucleation sites) on the surfaces of the SiNWs.

To test whether the oxide layer can also catalyze the formation of these carbon nanostructures, the as-synthesized SiNWs (sheathed with an oxide layer) were immersed in $CHCl_3$ and bath-sonicated in the same way. TEM results clearly showed that no carbon nanostructures were found. This experiment confirmed that the carbon nanostructures arose from the reactions between the SiH_x ($x = 1, 2, 3$) species on the surfaces of the SiNWs and the solvent molecules.

We also investigated the effect of ultrasonication on the reaction. The HF-etched silicon nanowires were dispersed in $CHCl_3$ and stirred for 15 min with a magnetic stirrer instead of bath sonication. While we also found some hydrocarbon nanostructures such as nanotubes and nano-onions, the quantities of these structures were far less than that obtained through bath sonication. Furthermore, the carbon structures are not as regular as that from bath sonication. This result indicates that ultrasonication plays an important role in the formation of these HCNTs/HCNOs. We believe that the chemical transformations on the surfaces of the SiNWs can be attributed to the fact that acoustic cavitation of ultrasound can induce local heating of up to temperatures as high as 5200 K and local pressures of several thousand atmospheres, with lifetimes of <1 μs.[18] Further-

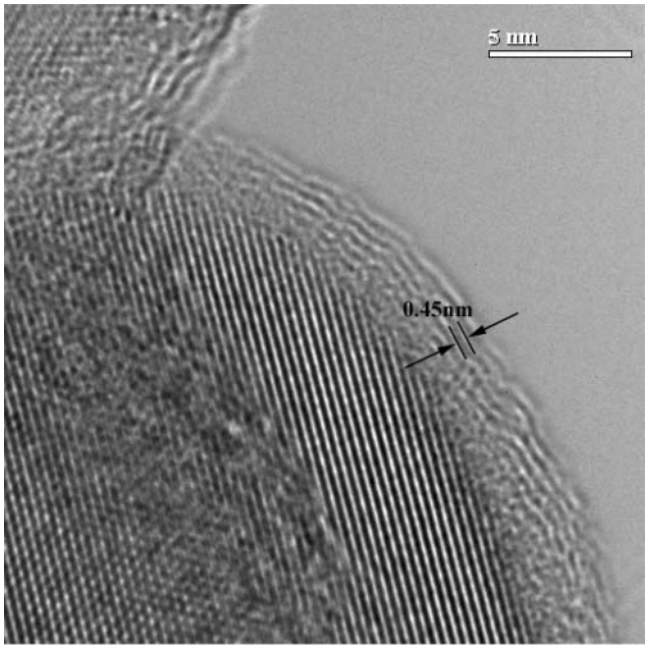

Figure 11. A HRTEM image of a close-up view of amorphous carbon layers on the surface of a SiNW and the continuous transformation of the amorphous carbon layers into wavy HCNTs with interlayer spacings of approximately 0.45 nm.

more, ultrasonication not only promotes the heterogeneous reaction between the SiH_x moieties on the SiNW surfaces and the organic molecules in solution but also facilitates the formation of the different types/shapes of carbon and hydrocarbon nanostructures as well as causes the extrusion (or demolding) of the products.

We propose the following mechanistic pathway for the formation of the HCNT(O)s/CNT(O)s. On the surfaces of the SiNWs, the chemisorbed organic solvent molecules react with the SiH_x moieties and, under the local high-temperature and high-pressure conditions within the ultrasound acoustic cavity[18] during the ultrasonication process, result in the elimination of the substituents of the solvent molecules. In the case of $CHCl_3$, the reaction between the Si−H and C−Cl bonds results in dehydrochlorination, giving rise to CH units which subsequently polymerize to form the hydrogenated graphite sheets[19] that wrap around the SiNWs (the templating effect). A closer look at Figure 9c reveals that there is a layer of amorphous carbon, measuring approximately 1 nm in thickness, between the SiNW surface and the HCNT. A more convincing picture is shown in Figure 11 which is the close-up view of an amorphous carbon layer on the surface of a different SiNW. It can be seen that, going outward from the surface of the SiNW, the amorphous carbon layer, with no discernible structure, begins to form fragmented layer structures. Strong spectroscopic evidence that corroborates this observation can be found in the three weak Raman peaks (as shoulders) at 1340, 1360, and 1370 cm^{-1} as discussed earlier. These bands are attributable to amorphous carbon or disordered graphite materials. This, we believe, is the genesis of the formation of the wavy layers of the HCNTs. While these heterogeneous reactions may be rather complicated, they may be represented as (eq 1)

$$(HC)_{ad} \xrightarrow[SiNW(D)]{sonication} a\text{-}(HC)_x \xrightarrow[SiNW(D)]{sonication} HCNT + HCNO \quad (1)$$

Here $(HC)_{ad}$ denotes the adsorbed hydrocarbon fragments on the surfaces of the SiNWs or silicon nanodots (SiNDs) (hereafter referred to collectively as SiNW(D)s) after the removal of the substituents (e.g., dehydrochlorination of $CHCl_3$) and a-$(HC)_x$ represents the polymerized amorphous hydrocarbons. These hydrocarbon polymer fragments may resemble hydrogenated amorphous carbon (a-C:H) on one hand and hydrogenated graphite on the other hand. The joining of the hydrogenated graphite fragments (the nucleation and growth processes) eventually forms wavy layers of HCNT(O)s that wrap around the SiNWs or SiNDs. Apparently, these reactions are facilitated and/or catalyzed by the sonication process and the active species on the surfaces of the SiNW(D)s.

Further sonication causes the SiNWs to shed off the HCNT(O)s, refreshing the SiNW surfaces for further reactions. The extruded HCNTs or HCNOs usually collapse to form different types of *solid* or *hollow* tubes or onions of various morphologies, depending on the types and shapes of silicon nanostructures (the template or mold). Snapshots of HCNTs as they were extruded from the SiNWs are portrayed in Figures 9 and 10. While these are examples of completely collapsed HCNTs upon extrusion from a SiNW, the majority of the HCNT products are hollow nanotubes.

We also found that, upon prolonged ultrasonication, the HCNT(O)s, with interlayer spacings greater than 3.4 Å, can be converted to the conventional CNT(O)s, with interlayer spacings of 3.4 Å, as represented in eq 2. Apparently these transformations involve dehydrogenation reactions (which may be catalyzed by the SiNW(D) templates), followed by the annealing process.

$$HCNT(O) \xrightarrow{sonication} CNT(O) \quad (2)$$

The nucleation and growth mechanism proposed here for the HCNT(O)s and CNT(O)s on SiNWs may be contrasted with the formation and growth of conventional carbon nanotubes, which have been studied extensively. For example, nucleation and growth mechanisms of carbon nanotubes from polyyne rings,[20] from two parallel carbon sheets via thermal activation,[21] or from a semifullerene nucleus,[22,23] as well as on a nanoparticle catalyst via a carbon precipitation process have been proposed.[24,25] As stated earlier, in our case, the carbon nanotube nucleation occurs at the active sites on the surfaces of the silicon nanowires. The active sites contain SiH_x species which, under the ultrasonication condition,[18]

(18) Suslick, K. S.; Price, G. J. *Annu. Rev. Mater. Sci.* **1999**, *29*, 295−326.
(19) Previous works by Nishihara, H., et al. (*J. Chem. Soc., Faraday* **1991**, *87*, 1187) showed that electrochemical reduction of halogenated organic compounds can lead to carbonaceous or graphitic deposits. These electrodeposited materials typically have a molecular structure resembling turbostratic graphite.
(20) Kiang, C. H.; Goddard, W. A., III. *Phys. Rev. Lett.* **1996**, *76*, 2515.
(21) Zhang, P.; Crespi, V. H. *Phys. Rev. Lett.* **1999**, *83*, 1791.
(22) Ge, M.; Sattler, K. *Science* **1993**, *260*, 515.
(23) Zhang, X. F.; Zhang, X. B.; Tendeloo, G. Van, Amelinckx, S.; Op de Beeck, M.; Van Landuyt, J. *J. Cryst. Growth* **1993**, *130*, 368.
(24) Saito, Y. *Carbon* **1995**, *33*, 979.
(25) Yudasaka, M.; Komatsu, T.; Ishihashi, T.; Achiba, Y.; Iijima, S. *J. Phys. Chem. B* **1999**, *102*, 4892.

promote the formation of the basic structural units of carbon source from the organic solvent. Polymerization of these basic units results in the formation of the graphene sheets which wrap around the SiNW (the mold). Further ultrasonication provides the energy needed for the dehydrogenation process, converting HCNT(O)s to CNT(O)s, as well as the extrusion of the nanotube from the SiNW mold. In this context, we note that carbon nanotube growth associated with metal particle catalysts has been proposed to occur by either a "root growth"[26] process, in which the nanotube base interfaces directly with the metal nanoparticles, or a "folded growth" mode,[27] in which the carbon shell that forms the nanotube wraps around the nanoparticles leading to the curved graphitic layers that extrude from the nanoparticle surface. On the basis of our TEM observations, the sonochemical growth of hydrocarbon or carbon nanotubes/onions on SiNWs reported here resembles more the "folded growth" mode. However, further work is needed to delineate details of the growth mechanisms.

Conclusion

In summary, a new type of hydrocarbon nanotubes and onions, with interlayer spacings ranging from 3.4 to 5.9 Å, was discovered by reacting SiNWs with common organic solvents in a laboratory ultrasonicator under ambient conditions (room temperature and atmospheric pressure). Along with these new nanostructures of carbon, the conventional CNT(O)s were also observed. The relative amount of the two types, HCNT(O)s vs CNT(O)s, depend on the starting materials and the experimental conditions (sonicating time, etc.).

A wide variety of topologies of hydrocarbon nanostructures can be observed, a collection of which is reported here. They include, but are not limited to, nanotubes (both solid and hollow ones); nano-onions (both solid and hollow); tubular networks, fused or patterned onions; open, closed, or connected loops or other networks; and twisted tubes or loops.

The templating effect (molding and demolding) of SiNWs or SiNDs, as well as the effect of the ultrasonication process, in the formation of the HCNT(O)s and CNT(O)s are discussed. A reaction/formation pathway for these carbon nanomaterials on silicon nanowire templates is proposed. Morphological and spectroscopic characteristics of the observed HCNT(O)s vs CNT(O)s are described and shown to be consistent with, and indeed provide strong evidence for, the proposed pathway.

Nucleation and growth mechanisms are also proposed for the observed HCNT(O)s and CNT(O)s and contrasted with the formation and growth of conventional carbon nanotubes advocated in the literature. Work is in progress to further our understanding of the reaction pathway(s) and/or mechanism(s) of these nanomaterials. New insights gained will have implications and significance in the future developments of the surface and materials chemistries of both carbon and silicon.

Acknowledgment. Financial support from a Central Allocation Grant (No. CityU 3/01C) of the Research Grants Council of Hong Kong (to S. T. Lee) is gratefully acknowledged. N. B. Wong acknowledges the support of a grant from the Research Grants Council of Hong Kong SAR (SiNWs RGC Grant 9040879 (CityU 1024/03)). B.K.T. would like to express his most sincere gratitude for the kind hospitality of S.T.L., N.B.W., and their colleagues at AP and BCH which was extended to him during his sabbatical at the City University of Hong Kong in 2002 where this work was performed.

Supporting Information Available: TEM images for various shapes of hydrocarbon nanotubes and onions such as twisted tubes or loops, knots, embroidery-like, and other networks of HCNTs/HCNOs. This material is available free of charge via the Internet at http:// pubs.acs.org.

CM050355N

(26) Dai, H.; Rinzler, A. G.; Nikolaev, P.; Thess, A.; Colbert, D. T.; Smalley, R. E. *Chem. Phys. Lett.* **1996**, *260*, 471−475.
(27) Hester, J. R.; Louchev, O. A. *Appl. Phys. Lett.* **2002**, *80*, 2580−2582.